To appear in the *Journal of Hydraulic Research*
Vol. 00, No. 00, Month 20XX, 1–26

Research paper

Viscoelastic models for the simulation of transients in polymeric pipes

Marco Ferrante, *Dipartimento di Ingegneria Civile ed Ambientale, University of Perugia, Via G. Duranti, 93 - 06125 Perugia, Italy*
Email: marco.ferrante@unipg.it (author for correspondence)

Caterina Capponi, *Dipartimento di Ingegneria Civile ed Ambientale, University of Perugia, Via G. Duranti, 93 - 06125 Perugia, Italy*
Email: caterina.capponi@studenti.unipg.it

Running head: Viscoelastic models for the simulation of transients.

ABSTRACT
In this paper simple viscoelastic models are implemented to asses their reliability in the simulation of transients in polymeric pipes. Two approaches are followed, i.e. the combination of elastic and viscous elements based on ordinary derivatives, and the use of fractional elements, based on fractional derivatives. The implementation of the viscoelastic component in an efficient numerical model, based on the frequency domain integration, allows the direct scrutiny of the optimization function used in the calibration and provides some general remarks about the viscoelastic parameter estimation. The numerical simulations are compared with the experimental data acquired during transient tests with pipes made of high density polyethylene (HDPE) and oriented polyvinyl chloride (PVC-O). The results show that the convergence toward the optimal solution depends in a different manner on the model parameters. The fractional model performs better than the others, although further studies are needed to verify its reliability and efficiency.

Keywords: Fractional derivatives; frequency domain; HDPE; PVC-O; transients; viscoelasticity.

1 Introduction

The widespread use of polymeric pipes in water distribution systems has increased the interest in the rheology of pipe materials. At least two issues related to the design and management have been investigated in the literature: the head-leakage relationship and the pressure wave propagation during transients.

Relating to the first issue, laboratory experiments and FEM models have shown that the leak area can vary with the pressure head and that the deformations are influenced by the pipe material characteristics (Cassa, van Zyl, & Laubscher, 2010; Ferrante, 2012; Ferrante, Massari, Brunone, & Meniconi, 2011; van Zyl & Cassa, 2013). As a result, in polyethylene and polyvinyl chloride pipes, under some circumstances, the leakage can depend on the pressure time history due to the viscoelastic behavior of the pipe materials (Ferrante et al., 2011; Fox, 2016; Massari, Ferrante,

Submitted on: June 2016

Brunone, & Meniconi, 2012; Ssozi, Reddy, & van Zyl, 2016).

Relating to transients, the governing equations of the unsteady flow in pressurized pipes require the definition of a stress-strain relationship that depends on the pipe material rheology (Covas et al., 2005, 2004; Ghilardi & Paoletti, 1987; Lee, Duan, Ghidaoui, & Karney, 2013; Pezzinga et al., 2014; Pezzinga & Scandura, 1995; Soares, Covas, & Reis, 2008; Suo & Wylie, 1989; Tijsseling, 1996; Weinerowska-Bords, 2006). Since transients are increasingly used as a diagnostic tool for pressurized pipe systems, reliable models of pipe material rheology play an important role in water system management (Duan, Lee, Ghidaoui, & Tung, 2012; Evangelista, Leopardi, Pignatelli, & de Marinis, 2015; Gong, Zecchin, Lambert, & Simpson, 2016; Kim, 2007; Kim, Zecchin, & Choi, 2014; Lee, Duan, Tuck, & Ghidaoui, 2015; Soares, Covas, & Reis, 2011; Vítkovský, Lee, Zecchin, Simpson, & Lambert, 2011).

Although they are also known as “plastics”, polymers behave as both viscous and elastic materials. Two main approaches can be used to describe such an intermediate response. The first one is based on the definition of two basic elements, elastic and viscous, and on their combination in series and parallels to reproduce complex intermediate models. The second one is based on the consideration that the viscosity law is characterized by an order one derivative in time and the elasticity law is based on an order zero derivative. As a consequence, a model based on a fractional derivative, i.e. a derivative of real order between zero and one, can describe a behavior between elastic and viscous and hence can be the basis of a viscoelastic model (Di Paola, Pirrotta, & Valenza, 2011).

In previous papers the effects of the pipe material on leak laws have been analyzed by means of experimental tests, comparing different elastic and viscoelastic models (Ferrante et al., 2011; Massari et al., 2012). In this paper the effects of pipe material on transients are investigated and different rheological models are used to simulate transients in polymeric pipes. In the first part, simple viscoelastic elements are presented and implemented in a numerical model based on the frequency domain integration of the governing equations. An element based on fractional derivatives is also introduced. In the second part, the experimental data acquired during transients in two systems with different materials, i.e. high density polyethylene (HDPE) and oriented polyvinyl chloride (PVC-O), are compared with the results of the numerical models. The used frequency domain integration reduces the computational burden and allows the analysis of the model calibration in a wide region of the parameter space.

The analysis of the calibration procedure by the direct scrutiny of the optimization function, the introduction of a fractional model, and the comparison of the viscoelastic models for two materials, in similar experimental set-up and test conditions, are the original contributions of this paper.

2 Viscoelastic models

The most established practice in the definition of the pipe material rheology is based on the combination of simple elements governed by ordinary differential equations. Fractional derivatives can also be used, leading to a different category of elements. These two approaches are discussed in the following.

2.1 *Combination of springs and dashpots*

A viscoelastic material, presenting both elastic and viscous characteristics, can be modeled as a combination of linear elastic and linear viscous elements.

For a linear elastic body, the dependence of the stresses, σ, on the strains, ϵ, (or Hooke's law) is:

$$\sigma(t) = E\frac{\mathrm{d}^0\epsilon(t)}{\mathrm{d}t^0} = E\epsilon(t) \tag{1}$$

where t is the time and E is the Young's modulus. The simple ideal element following this law is a *spring*.

For a linear viscous fluid, the dependence of the stress on the first derivative of the strain (or Newton's law) is given by:

$$\sigma(t) = \eta\frac{\mathrm{d}^1\epsilon(t)}{\mathrm{d}t} = \eta\frac{\mathrm{d}\epsilon(t)}{\mathrm{d}t} \tag{2}$$

where η is the viscosity coefficient. The simple ideal element governed by this law is a *dashpot*.

A series of a spring with a dashpot is the so called *Maxwell* element (MX), while a parallel of a spring with a dashpot is the so called *Kelvin-Voigt* element (KV). For the Maxwell element it is:

$$\frac{1}{E_{MX}}\frac{\mathrm{d}\sigma}{\mathrm{d}t} + \frac{\sigma}{\eta_{MX}} = \frac{\mathrm{d}\epsilon}{\mathrm{d}t} \tag{3}$$

while for the Kelvin-Voigt element it is:

$$\sigma = E_{KV}\epsilon + \eta_{KV}\frac{\mathrm{d}\epsilon}{\mathrm{d}t} = E_{KV}\left(\epsilon + \tau_{KV}\frac{\mathrm{d}\epsilon}{\mathrm{d}t}\right) \tag{4}$$

where $\tau = \eta/E$, and the subscripts denote the model. These simple combinations of the springs and dashpots can partially reproduce the viscoelastic behavior during creep (relaxation) tests, where the strain (stress) variation in time is measured for a constant applied stress (strain). As an example, the KV model can reproduce the creep of a material but it is inadequate to simulate the relaxation tests (e.g., Di Paola et al., 2011). On the opposite, the MX model can be reliably applied to model relaxation tests while it is inadequate for creep tests. To avoid the physical inadequacy of the Kelvin-Voigt element, it is coupled in series with a spring. The resulting model is usually referred to as *Standard Linear Solid* (SL) or *Zener* model.

The models obtained by combinations of springs and dashpots can always be described in a general form by an ordinary differential equation:

$$\sum_{k=0}^{n} a_k \frac{\mathrm{d}^k\sigma(t)}{\mathrm{d}t^k} = \sum_{k=0}^{m} b_k \frac{\mathrm{d}^k\epsilon(t)}{\mathrm{d}t^k} \tag{5}$$

where $k \in \mathbb{N}$, and a and b are model parameters. Hence, following the element combination approach, the variation in time of stresses and strains is defined in terms of exponential functions.

2.2 *Fractional models*

Another way to define an intermediate behavior between elastic and viscous, i.e. between Eqs (1) and (2), is based on the consideration that these limit conditions are described by a zero and a first derivative. Hence, a viscoelastic model can be defined by a derivative of order $0 \leq \theta \leq 1$:

$$\sigma(t) = k_\theta \frac{\mathrm{d}^\theta\epsilon(t)}{\mathrm{d}t^\theta} \tag{6}$$

The simple ideal element following this law is a *springpot*, also referred to as *fractional* element.

The approach based on fractional derivatives has not been used in the past as widely as the one based on the combination of elementary models to describe viscoelastic behaviors. One reason for this preference can be the physical meaning of the fractional derivatives. As a matter of fact, in the

Newtonian mechanic laws only integer order derivatives appear, for both governing equations and boundary conditions. While the derivatives in time of order 1 or 2 can be associated to velocity and acceleration, it is difficult to associate a physical quantity to a derivative of order 1/3. With specific reference to the rheology, while E, η and τ have an intuitive physical meaning, the same does not apply to the parameter k_θ.

A theoretical basis for the application of fractional calculus to viscoelasticity has been introduced by Bagley and Torvik (1983) considering the molecular theory for dilute polymer solutions. Another interesting attempt to overcome this limitation has been proposed by Schiessel and Blumen (1993, 1995) and it is based on the consideration that an infinite number of springs and dashpots combined in a ladder arrangement can be associated with one springpot. In general, the statistical interpretation of arrangements of a large number of springs and dashpot takes to fractional derivatives and springpots. Hence, intuition suggests that a single fractional element could represent a series of many springs and dashpots. Moreover, Di Paola et al. (2011) have shown that a single springpot element can interpret both relaxation and creep tests.

Another disadvantage in using the fractional derivatives comes from the different ways they have been defined. A complete discussion of the possible choices and on the limitations in using the Riemann-Liouville or the Caputo fractional derivative is beyond the scope of this paper. Interested readers can find details in textbooks and papers (e.g.: Gorenflo & Mainardi, 2007; Mainardi, 2010; Shimizu & Zhang, 1999). What is important to remark here, is that derivatives of integer order can be obtained as singular cases of real order derivatives, as integers are contained in the real domain. Furthermore, the definition allows the extension to real derivatives of some interesting properties that apply to integer derivatives. Considering the Fourier transform of a fractional derivative of a generic function of time, $g(t)$, it is:

$$\mathscr{F}\{\frac{\mathrm{d}^\theta g(t)}{\mathrm{d}t^\theta};\omega\} = (i\omega)^\theta\,\mathscr{F}\{g(t);\omega\} \tag{7}$$

where $\mathscr{F}\{\cdot;\omega\}$ denotes the Fourier transform, ω is the angular frequency and $i=\sqrt{-1}$.

The general fractional model (Caputo & Mainardi, 1971) corresponding to Eq. (5) is:

$$\sigma + k_\iota\frac{\mathrm{d}^\iota\sigma(t)}{\mathrm{d}t^\iota} = E_0\epsilon + k_\theta\frac{\mathrm{d}^\theta\epsilon(t)}{\mathrm{d}t^\theta} \tag{8}$$

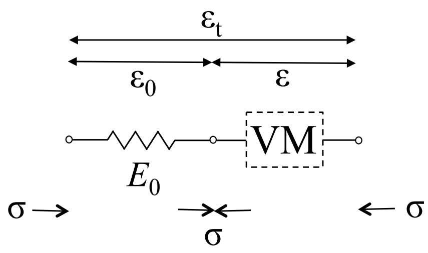

Figure 1: The implemented rheological models consist of a spring with Young's modulus E_0 in series with other elements (VM). The total hoop strain, ϵ_t, is the sum of the spring strain, ϵ_0, and the strain of VM, ϵ.

where $\theta = \iota$ as introduced by Caputo and Mainardi (1971) and explained in (Bagley, 1986) by thermodynamic constraints. The remarkable result is that relaxation tests governed by this equation can be explained by power laws instead of exponential laws (Di Paola et al., 2011). In the following, a simplified model is used, assuming $k_\iota = 0$ in Eq. (8), i.e.:

$$\sigma = E_0\epsilon + k_\theta \frac{\mathrm{d}^\theta \epsilon(t)}{\mathrm{d}t^\theta} \tag{9}$$

Since this model corresponds to an MX model with a springpot instead of the dashpot, it is usually referred to as Generalized Maxwell model (GM).

3 Equations of unsteady flow in viscoelastic pipes

In the following we assume that the pipe material rheological model is made of a spring, with Young's modulus E_0, in series with the remaining part of the model, referred to as VM in the following (Fig. 1). Due to the series arrangement, the total hoop strain can be considered as the sum of two terms, $\epsilon_t = \epsilon_0 + \epsilon$ where ϵ_0 corresponds to the spring strain component while ϵ denotes the strain associated to VM. For the same reason, the same stress $\sigma = \epsilon_0 E_0$ is applied to the spring and VM. Under this and the other common assumptions (Chaudhry, 2014; Wylie & Streeter, 1993), the equations governing the one-dimensional transient flow are:

$$\begin{aligned} C\frac{\partial H}{\partial t} + \frac{\partial Q}{\partial x} + 2A\frac{\partial \epsilon}{\partial t} &= 0 \\ L\frac{\partial Q}{\partial t} + \frac{\partial H}{\partial x} + R'Q|Q| - B\frac{\partial Q}{\partial x} &= 0 \end{aligned} \tag{10}$$

where Q is the discharge, H is the piezometric head, x is the spatial coordinate, A and D are the pipe cross-sectional area and diameter, respectively. The capacitance, $C = gA/a^2$, the inertance, $L = (2 + k_B)/(2gA)$, the steady resistance, $R = f/(2gDA^2)$, and the unsteady resistance, $B = ak_B/(2gA)$, are also introduced, where g is the gravitational acceleration, f is the friction factor and k_B is the Brunone's (1995) formula coefficient. For the sake of simplicity, the Brunone's formula is introduced in Eqs (10) although the effects of the unsteady-friction could be modeled in the more general framework provided by the convolution integral formulation (Weinerowska-Bords, 2015). Because of the systems considered in the following, the original unsteady-friction formula is used (Bergant, Simpson, & Vítkovský, 2001; Brunone et al., 1995).

Only the strain component ϵ_0 contributes to the evaluation of the wave speed, a. The term $2A\frac{\partial \epsilon}{\partial t}$ in Eqs (10) takes into account the characteristics of the remaining part of the rheological model, VM, in series with the spring.

The system of the two equations (10) with the two independent variables, x and t, relates three dependent variables, i.e. Q, H and ϵ. To solve the problem, a rheological model is introduced to relate ϵ to σ, which in turn si related to H by the Mariotte's formula:

$$\sigma = \lambda \frac{\rho g D}{2e} H = SH \tag{11}$$

In Eq.(11), λ is the pipe constraint coefficient, ρ is the water density and e is the the pipe wall thickness, with $e \ll D \ll H$.

As an example, for SL, the combination of Eqs (4) and (11) yields:

$$SH = E_{KV} \left(\epsilon + \tau_{KV} \frac{\mathrm{d}\epsilon}{\mathrm{d}t} \right) \tag{12}$$

To integrate in the frequency domain the set of the governing equations, a linearized form is obtained, considering the dependent variables H, Q and ϵ, as the sum of two components, a mean value and a perturbation:

$$Q = \bar{Q} + q^* \, , \; H = \bar{H} + h^* \, , \; \epsilon = \bar{\epsilon} + \varepsilon^* \tag{13}$$

If H, Q and ϵ are substituted with the mean values $\bar{H}$, $\bar{Q}$ and $\bar{\epsilon}$, Eqs (10) still hold. As an example, this applies to the steady state initial conditions or to slow variations of the variables in time, where the term "slow" means that the periods of the variation components are much larger than the time duration of interest.

As a result of this assumption, the perturbation equations corresponding to Eqs (10) can be derived:

$$\begin{aligned} C\frac{\partial h^*}{\partial t}+\frac{\partial q^*}{\partial x}+2A\frac{\partial \varepsilon^*}{\partial t} &=0 \\ L\frac{\partial q^*}{\partial t}+\frac{\partial h^*}{\partial x}+Rq^*-B\frac{\partial q^*}{\partial x} &=0 \end{aligned} \tag{14}$$

where the perturbation product q^*q^* is neglected and the term $R=\bar{Q}f/(gDA^2)$ is used instead of R'. The approxations introduced in the model as an effect of such a linearization are discussed by Capponi, Zecchin, Ferrante, and Gong (sub); Lee (2013); Lee and Vítkovský (2010).

Assuming that the generic perturbation, $y^*{=}y(x)e^{i\omega t}$, is the product of two terms taking into account the dependence on time and space separately or, in other words, taking the Fourier transform of Eqs (14), yields:

$$\begin{aligned} Ci\omega\, h+\frac{\mathrm{d}q}{\mathrm{d}x}+2Ai\omega\,\varepsilon &= 0 \\ (Li\omega+R)\,q+\frac{\mathrm{d}h}{\mathrm{d}x}-B\frac{\mathrm{d}q}{\mathrm{d}x} &= 0 \end{aligned} \tag{15}$$

The ε term can be evaluated by means of the Fourier transform of the equations corresponding to the chosen viscoelastic model. As an example, Eq.(12) becomes:

$$Sh = E_{KV}\,(1+\tau_{KV}i\omega)\,\varepsilon \tag{16}$$

Introducing the transformed equation in Eq. (15) and substituting for ε, a system of two equations is obtained:

$$\begin{aligned} \alpha h+\frac{\mathrm{d}q}{\mathrm{d}x} &=0 \\ \beta q+\frac{\mathrm{d}h}{\mathrm{d}x}-B\frac{\mathrm{d}q}{\mathrm{d}x} &=0 \end{aligned} \tag{17}$$

Table 1: Used viscoelastic models.

Model	Sketch	n_P	Parameters	$f(\omega)$
EL	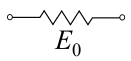	1	E_0	0
MX	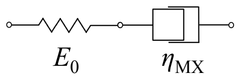	2	E_0, η_{MX}	$S/\left(i\omega\eta_{MX}\right)$
GM	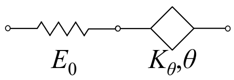	3	E_0, θ, k_θ	$S/\left[k_\theta(i\omega)^\theta\right]$
SL	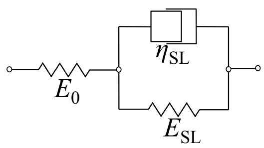	3	E_0, E_{SL}, η_{SL}	$S/\left(E_{SL} + i\omega\eta_{SL}\right)$

where:

$$\begin{aligned} \alpha &= i\omega\left[C + 2Af(\omega)\right] \\ \beta &= \left[Li\omega + R\right] \end{aligned} \tag{18}$$

The function $f(\omega)$ depends on the chosen rheological model of the pipe material. For a linear elastic material it is $f(\omega) = 0$. In Table 1 the $f(\omega)$ formulae are given for different rheological models. In the same table the model parameters are also specified. The use of different rheological models modifies the expression of α by $f(\omega)$ but not β. This is because only the first of Eqs (17), i.e. the continuity equation, depends on the rheological model. On the contrary, the used unsteady-friction model affects the evaluation of L and introduces an asymmetry in the set of equations.

The introduction of the fractional derivatives in the set of equations does not require any further manipulation or approximation. In fact, due to the properties of the Fourier transform of the fractional derivatives of Eq. (7), the simple relationship can be derived:

$$Sh = k_\theta \left(i\omega\right)^\theta \varepsilon \tag{19}$$

and hence $f(\omega) = S/[k_\theta(i\omega)^\theta]$. With respect to the other considered models, in this case α depends on a real power of ω and hence the use of the fractional derivatives introduces a different functional expression in $f(\omega)$.

Following the so called Impedance Response method (Chaudhry, 2014; Wylie & Streeter, 1993) and introducing the impedance $Z = h(x)/q(x)$, the integration of Eqs (17) for the case of a Reservoir-Pipe-Valve (RPV) system gives (Kim, 2005):

$$Z_D = Z_{C1} Z_{C2} \frac{-\mathrm{e}^{\gamma_1 L_T} + \mathrm{e}^{-\gamma_2 L_T}}{Z_{C2}\mathrm{e}^{\gamma_1 L_T} + Z_{C1}\mathrm{e}^{-\gamma_2 L_T}} \tag{20}$$

where Z_D is the pipe downstream end impedance, $Z_{C1} = \gamma_1/\alpha$, $Z_{C2} = \gamma_2/\alpha$, $\gamma_1 = (-\alpha B + \Delta)/2$, $\gamma_2 = (\alpha B + \Delta)/2$, $\Delta = \left(\alpha^2 B^2 + 4\alpha\beta\right)^{1/2}$ and L_T is the length of the pipe.

A further simplification can be obtained if the unsteady-friction term is neglected and $k_B = B = 0$. In this case it is $\gamma_1 = \gamma_2 = \gamma = (\alpha\beta)^{1/2}$, $Z_{C1} = Z_{C2} = Z_C = (\beta/\alpha)^{1/2}$ and Eq. (20) simplifies in:

$$Z_D = -Z_C \tanh(\gamma L_T) \tag{21}$$

Since the Fourier transform of the pressure head variation at the downstream end of the pipe, $\mathscr{F}\{\Delta H_D; \omega\}$ is the product of Z_D with the Fourier transform of the discharge variation $Z_Q = \mathscr{F}\{\Delta Q_D; \omega\}$ (Ferrante & Brunone, 2003; Lee et al., 2015), the time history of ΔH_D can be determined by an inverse Fourier transform once ΔQ_D is known.

The integration of the Eqs (10) in the frequency domain and the use of Eqs (20) and (21) dramatically reduces the computational burden required for each simulation with respect to the time domain integration methods, e.g. the method of characteristics. For this and for other reasons, frequency domain based approaches are used for complex systems (Kim, 2007, 2016; Zecchin, Lambert, & Simpson, 2010; Zecchin, Simpson, & Lambert, 2009). In the following the results of the numerical model based on Eqs (20) and (21) are used to estimate the optimal values of the viscoelastic parameters of polymeric pipes by the comparison with transient test data.

Table 2: Distances of pressure transducers PT_U, PT_{IU}, PT_{ID}, PT_D and of the motorized valve MV from the upstream pressure vessel R in the experimental set-up (Fig. 2). For full scales of the pressure transducers (f.s.), G denotes gauge while A denotes absolute pressure.

Material	x	PT_U	PT_{IU}	PT_{ID}	PT_D	MV
	x(m)	1.00	33.49	82.39	101.88	L_T =102.58
HDPE	f.s. (bar)	7 (G)	7 (G)	7 (G)	5 (G)	
	accuracy (% of f.s.)	0.25	0.25	0.25	0.15	
	x(m)	0.40	33.06	83.08	104.68	L_T =105.30
PVC-O	f.s. (bar)	7 (G)	5 (A)	5 (A)	5 (A)	
	accuracy (% of f.s.)	0.25	0.25	0.25	0.15	

4 Experimental apparatus and tests

The tests were carried out at the Water Engineering Laboratory of the University of Perugia, Italy, on two RPV systems, differing for the pipe material.

In both systems at the upstream end of the pipe there was an air vessel, R, while at the downstream end there was a hand-operated ball valve, DV, discharging into the air and a remotely controlled butterfly valve, MV, immediately upstream of DV (Fig. 2). An electromagnetic flowmeter, FM, was used to measure the discharge during the steady-state initial conditions, with an accuracy of 0.2% of the measured value. Four piezoresistive pressure transducers were used to measure the pressure in the pipe close to the reservoir (PT_U), upstream of the maneuver valve (PT_D) and at two intermediate measurement sections (PT_{IU} and PT_{ID}). Pressure transducers locations and characteristics where slightly different for the two systems (Table 2). A further piezoresistive pressure transducer (f.s. 10 bar, accuracy of 0.25% f.s.) was used to measure the pressure in R.

In the first system, an oriented polyvinyl chloride (PVC-O) DN110 PN16 pipe was used, according to ISO 16422 and NFT 54-948, of length L_T = 105.30 m, with an internal diameter D = 103.0 mm and a wall thickness e = 2.7 mm. Preliminary results on the same set-up are shown in (Ferrante, Capponi, Brunone, & Meniconi, 2015).

In the second system a high density polyethylene (HDPE) DN110 PN10 pipe was used, according to UNI EN 12201 and UNI EN ISO 15494, of length L_T = 102.58 m, with an internal diameter D = 96.8 mm and a wall thickness e = 6.6 mm.

Two transient tests were generated in the two systems by means of a complete and fast closure maneuver and are analyzed in the following. By means of the appropriate combination of the initial opening degrees of DV and MV, it was possible to obtain similar initial steady-state conditions and overpressures in the two systems. For the PVC-O system the initial discharge Q_0 = 3.70 l/s corre-

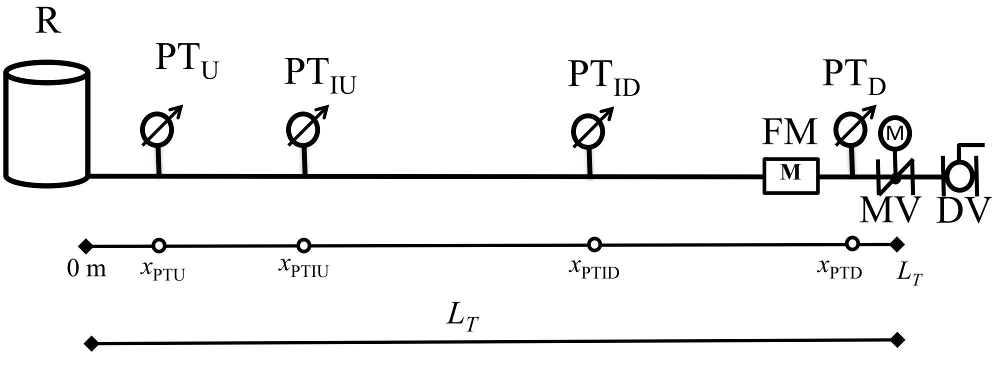

Figure 2: The laboratory set-up. R is the upstream air vessel, PT_X denotes a pressure transducer, FM is the flow meter, MV and DV are the remotely controlled butterfly valve and the hand operated ball valve, respectively. Distances are given in Table 2.

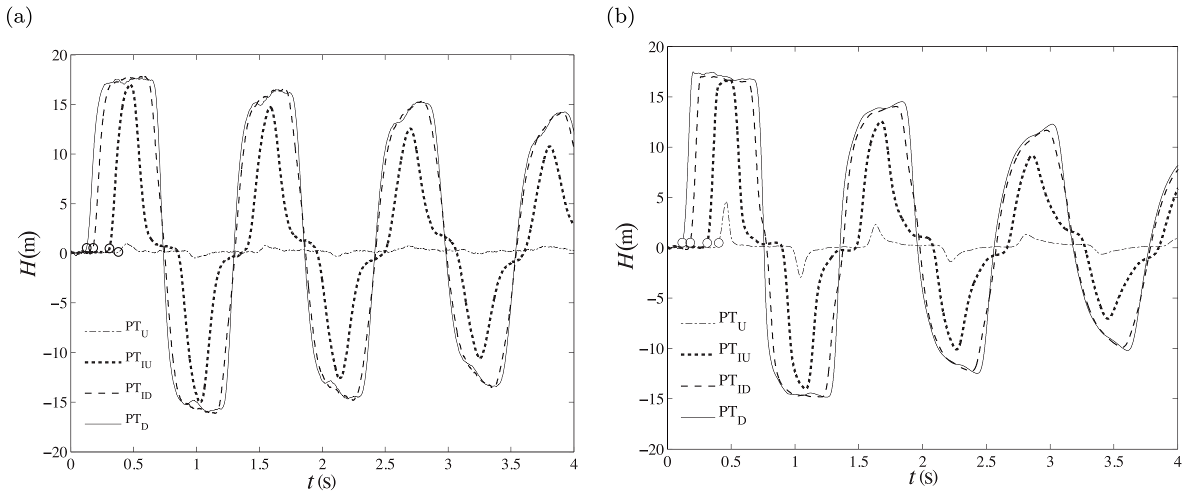

Figure 3: Measured pressure signals acquired by the pressure transducers on (a) PVC-O and (b) HDPE. Hollow circles denote the arrival times at the measurement sections of the first pressure wave traveling from MV to R.

sponded to a Reynolds number $\mathsf{R}_0 = 45740$ while for HDPE it was $Q_0 = 3.64$ l/s and $\mathsf{R}_0 = 47880$.

The obtained variations in time of the piezometric head, or pressure signals, acquired at the frequency of 100 Hz at the four measurement sections (PT_U, PT_{IU}, PT_{ID}, and PT_D) are shown in Figures 3a and 3b, for PVC-O and HDPE, respectively. In these figures, as well as in the following, the pressure signals are referred to the piezometric head in the air vessel R, which was almost constant during the tests and equal to 21.5 and 20.0 m for PVC-O and HDPE, respectively.

The different rheological behavior of the two polymeric materials reflects in different periods and pressure amplitude damping over the experiment duration.

5 Numerical simulations

To fit the experimental data by means of a numerical model based on Eqs (20) or (21), the discharge variation at the downstream end, ΔQ_D, and a set of values of the viscoelastic parameters must be provided. To define ΔQ_D, a hyperbolic function:

$$\frac{\Delta Q_D}{Q_0} = \frac{1}{2}\left[1 - \tanh\left(k_1 t - k_2\right)\right] \tag{22}$$

has been fitted to the experimental data so that the numerical model reproduces with a good agreement the raising limb of the pressure signals in the first characteristic time (Brunone & Morelli, 1999). For both systems the values of the two parameters k_1=32 s^{-1} and k_2= 5.5 have been used. The estimated flow variation at the valve was then introduced in the numerical model at the downstream end node to simulate the maneuver of MV.

To evaluate the viscoelastic parameters for each model, a calibration is performed based on the fitting of the the numerical results to the measured data. As a measure of the fitting reliability, i.e. of the distance between the numerical model results and the experimental data, the sum of the squared errors:

$$\sigma^2 = \frac{\sum_{i=1}^{n}\left(H_i - \hat{H}_i\right)^2}{n} \tag{23}$$

is used, where n is the number of samples and H_i ($\hat{H}_i$) is the i-th piezometric head value simulated (measured) at $\mathrm{PT_D}$.

To calibrate the models, i.e. to define the optimal set of the parameter values which minimizes the optimization function σ^2, two steps are considered. In the first step, σ^2 is calculated on a regular grid in the space of the parameters and a minimum value is obtained by the direct scrutiny of the grid data. As a second step, a minimum search algorithm is used to determine the optimal values of the parameters, starting from the grid minimum solution. This particular way of examining the optimization function is made possible by the reduced computational burden of the used transient simulation model. The provided shape of the optimization function over a large range of the parameter values suggests some general remarks on calibration techniques.

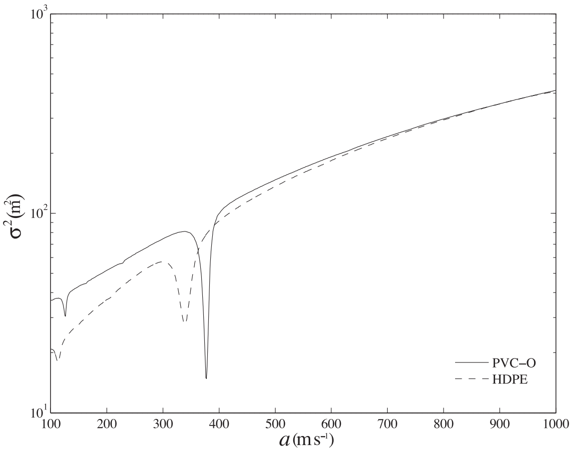

Figure 4: EL model - Variation of σ^2 with a for PVC-O and HDPE.

5.1 *The elastic model EL and the effects of the unsteady-friction*

The implementation of the elastic rheological element produces the simplest model among those considered in this work.

In Fig. 4 the variation of σ^2 with a is shown for both PVC-O and HDPE pipes. In both cases the function σ^2 has two local minima in the considered range of variation of a. For the test on the PVC-O pipe (solid line), the global minimum of σ^2 is for a = 377.4 m/s while the other local minimum is for a =377.4/3=125.8 m/s. The value corresponding to the global minimum is close to that associated to the speed of the first wave traveling from MV to R. In fact, assuming that the wave arrival times at the measurement sections correspond to those pointed out by hollow circles in Fig. 3a, a mean value of 405.0 m/s can be obtained.

For the test on the HDPE pipe (dashed line) the global minimum corresponds to the lowest value, i.e. 112.9 m/s, and not to the more reasonable value of 338.8 m/s, closer to the value of 352.0 m/s estimated by means of the wave arrival times pointed out by hollow circles in Fig. 3b and associated to the other local minimum.

The term *wave speed* is here clearly associated to the parameter a, which is determined by calibrations and is constant in time. Other definitions can be used in a quantitative and qualitative manner to describe the actual traveling wave speed (Tijsseling & Vardy, 2015). The used definition and the difficulties in defining the actual arrival times can explain the differences between a and the estimated first wave speed.

The reasons of the two minima and the behaviour of σ^2 for the HDPE system in Fig. 4 are explained in Fig. 5b where the simulated pressure signals corresponding to the optimization function minima are compared to the experimental results. The damping due to the viscoelastic effect cannot be interpreted by the implemented elastic model and hence the value of a that reproduces the correct number of periods (a =338.8 m/s) systematically overestimates the acquired signal. On the contrary, a simulation with a wave speed reduced to a =338.8/3 $\simeq$ 112.9 m/s produces a signal with a lower damping, underestimating the measured value for the first duration. As a result, the smallest value of a yields a reduced value of σ^2 with respect to what can be defined the correct one. In fact, considering a =112.9 m/s as the optimal value corresponds to affirm that a not working clock is more accurate than a clock 10 minutes late, since it is able to reproduce the correct time two times per day. In terms of calibration procedure, the chosen optimization function does not penalize a wrong number of periods and the mistake is introduced in the used measure of the distance between simulated and experimental data.

In Fig. 5a, two numerical signals obtained by the calibrated EL model are compared to the experimental one (EXP) for the PVC-O system. For the first one (EL), the unsteady-friction effects have been neglected ($k_B = 0$). For the second one (EL+UF), the unsteady friction effects are evaluated with $k_B = 0.005$ as determined by means of the diagrams in (Pezzinga, 2000). Based on the comparison of these two numerical signals, the considered test conditions (Duan, Ghidaoui, & Lee, 2010; Duan et al., 2012), and the aims of this paper, the unsteady-friction effects are considered as negligible and are not included in the following simulations.

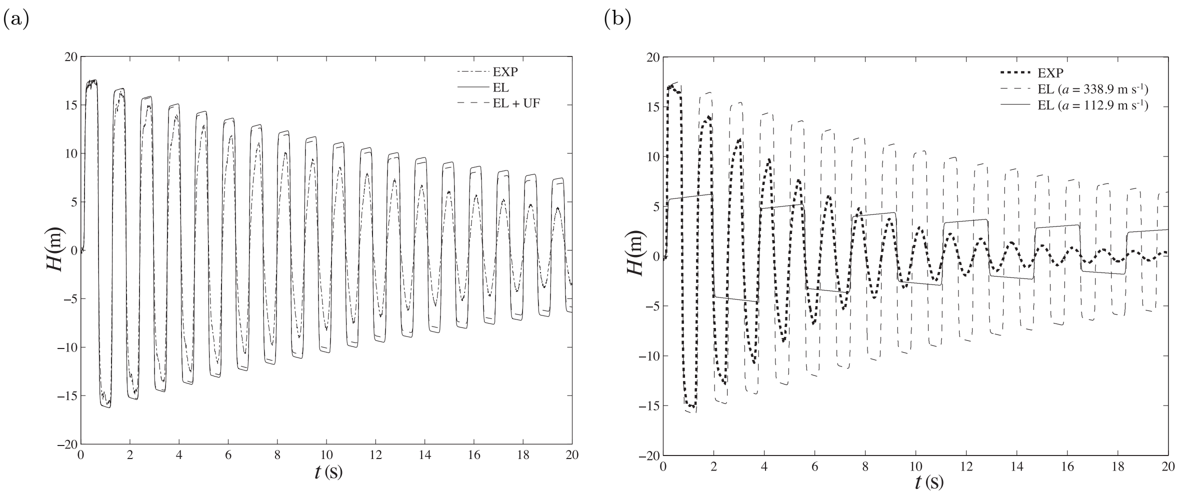

Figure 5: Comparison of the measured and simulated values (EL model) of H at $\mathrm{PT_D}$ for (a) PVC-O and (b) HDPE.

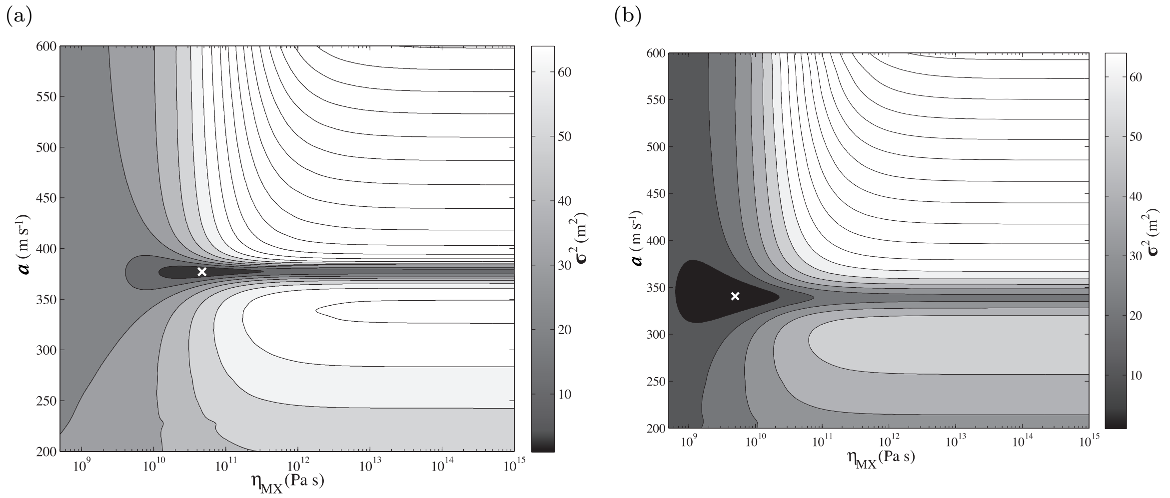

Figure 6: MX model - Variation of σ^2 with a and η_{MX} for (a) PVC-O and (b) HDPE.

5.2 *The Maxwell model, MX*

In Fig. 6 the variation of σ^2 with the two parameters of the MX model, a and η_{MX}, is shown for PVC-O and HDPE. Due to the considered variation range, a logarithmic scale is used for the η_{MX} axis. For both the materials, σ^2 depends on the two parameters in a completely different manner. While for a given value of η_{MX} from 10^{10} to 10^{15} Pa s the optimal values of a are similar and close to the global minimum, the same does not apply for a given value of a and the corresponding optimal value of η_{MX}. As a result, we expect that while in an optimization procedure any reasonable initial value of η_{MX} leads to similar values of a, close to the optimal one, the search for the optimal η_{MX} value is not as easy.

Using the minimum value of σ^2 on the 100 by 100 grid as a starting point and applying a non linear minimum search algorithm, the optimal values of $a = 377.1$ and 340.7 m/s, and $\eta_{MX} = 4.68\ 10^{10}$ and $5.00\ 10^9$ Pa s are obtained for PVC-O and HDPE, respectively. The solutions corresponding to these values are pointed out by white crosses in Fig. 6 and are used to simulate the numerical results of Fig. 9 (dashed line).

5.3 *The Standard Linear Solid model, SL*

To simplify the representation of the results of the SL model, in Fig. 7 a slice of the optimization function for the optimal value of a is shown in the plane of the two parameters, E_{SL} and η_{SL}, for PVC-O (Fig. 7a) and HDPE (Fig. 7b). In these figures, the lines corresponding to the same value of τ_{SL} are also shown and the axes are both in logarithmic scale.

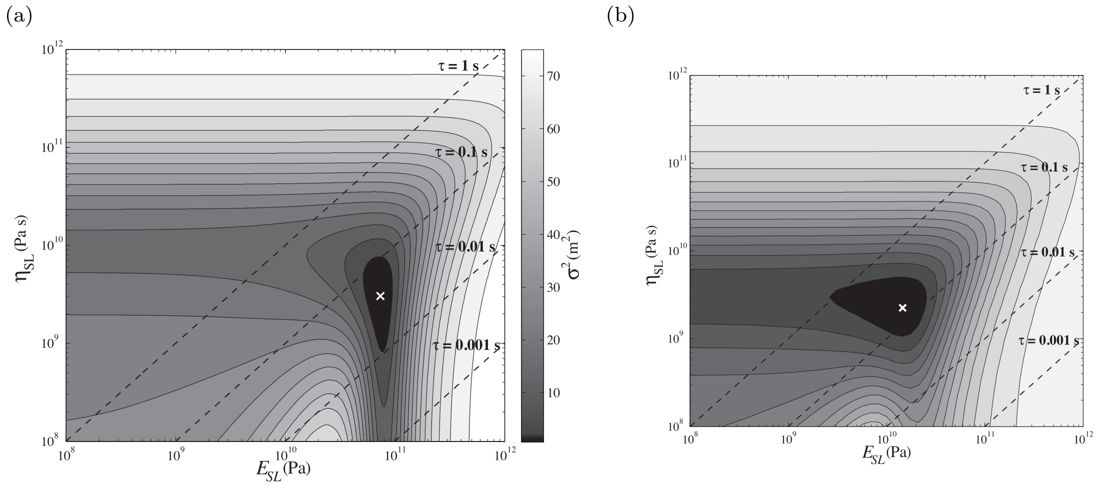

Figure 7: SL model - Variation of σ^2 with E_{SL} and η_{MX} for (a) PVC-O and (b) HDPE, for a=390.7 m/s.

For PVC-O, the optimal values of a=390.7 m/s, $E_{SL} = 7.688\ 10^{\ 10}$ Pa and $\eta_{SL} = 3.3361\ 10^9$ Pa s, are denoted by a white cross in Fig. 7a and correspond to $\tau_{SL} = 0.0434$ s. For HDPE, the optimal values of a=351.4 m/s, $E_{SL} = 1.456\ 10^{\ 10}$ Pa and $\eta_{SL} = 2.252\ 10^9$ Pa s, also denoted by a white cross in Fig. 7b, correspond to $\tau_{SL} = 0.155$ s.

The dependence of σ^2 on the two considered parameters in Fig. 7 is not as simple as that of Fig. 6 and curves corresponding to the same value of σ^2 are parallel to one of the axis or to the other one, depending on the considered range of variation of the parameter.

5.4 *The Generalized Maxwell model, GM*

Figures 8a and 8b show the dependence of the optimization function on two of the calibration parameters, θ and k_θ, for the optimal value of a, for the PVC-O and the HDPE pipe, respectively.

For k_θ, a range of variation over several orders of magnitude is considered, comparable to those used for E and η, for the other models. On the opposite, only the interval from 0 (elastic) to 1 (viscous) is considered for θ. An investigation of the model behavior outside of this range confirmed that a derivative of order greater then one does not provide a good fitting to the experimental data. The limited range of θ is an advantage in the calibration procedure.

The optimal values of θ=0.0537 and 0.1874 for PVC-O and HDPE, respectively, suggest that PVC-O is closer to an elastic material (θ=0) than the HDPE. The optimal values of k_θ=2.3203 10^{10} Pa s$^\theta$ and 6.2926 10^9 Pa s$^\theta$ are between the corresponding values of E_{SL} and η_{SL} for both materials.

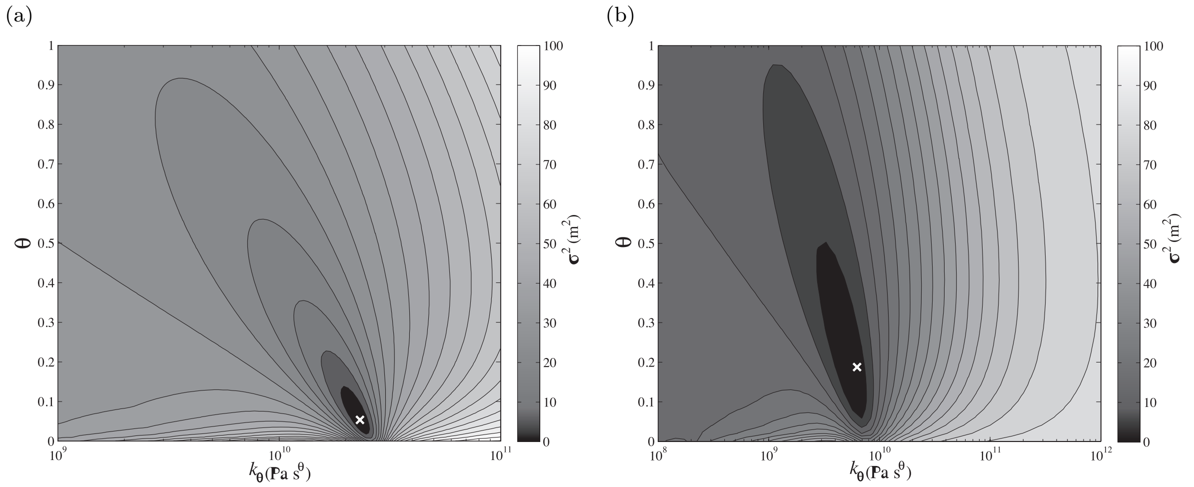

Figure 8: GM model - Variation of σ^2 with k_θ and θ for (a) PVC-O and (b) HDPE, for a=424.6 and 376.54 m/s, respectively.

Table 3: Results of the model calibration with the experimental data on PVC-O.

Model	σ^2	Parameters	
EL	14.694 m^2	a	377.4 m/s
MX	2.103 m^2	a	377.1 m/s
		η_{MX}	4.680 10^{10} Pa s
SL	0.6783 m^2	a	390.7 m/s
		E_{SL}	7.376 10^{10} Pa
		η_{SL}	3.047 10^9 Pa s
GM	0.6509 m^2	a	424.6 m/s
		θ	0.0537
		k_θ	2.3203 10^{10} Pa s$^\theta$

Table 4: Results of the model calibration with the experimental data on HDPE.

Model	σ^2	Parameters	
EL	27.762 m^2	a	338.8 m/s
MX	1.205 m^2	a	340.7 m/s
		η_{MX}	4.500 10^9 Pa s
SL	0.3719 m^2	a	351.4 m/s
		E_{SL}	1.4559 10^{10} Pa
		η_{SL}	2.2517 10^9 Pa s
GM	0.3282 m^2	a	376.5 m/s
		θ	0.1874
		k_θ	6.2926 10^9 Pa s$^\theta$

6 Discussion of the results

The obtained results for PVC-O and HDPE are summarized in Tables 3 and 4, respectively. The calibration of the EL model confirms once again that, for the polymeric materials, an elastic rheological model cannot reproduce the pressure signals during transients. In fact, even if the

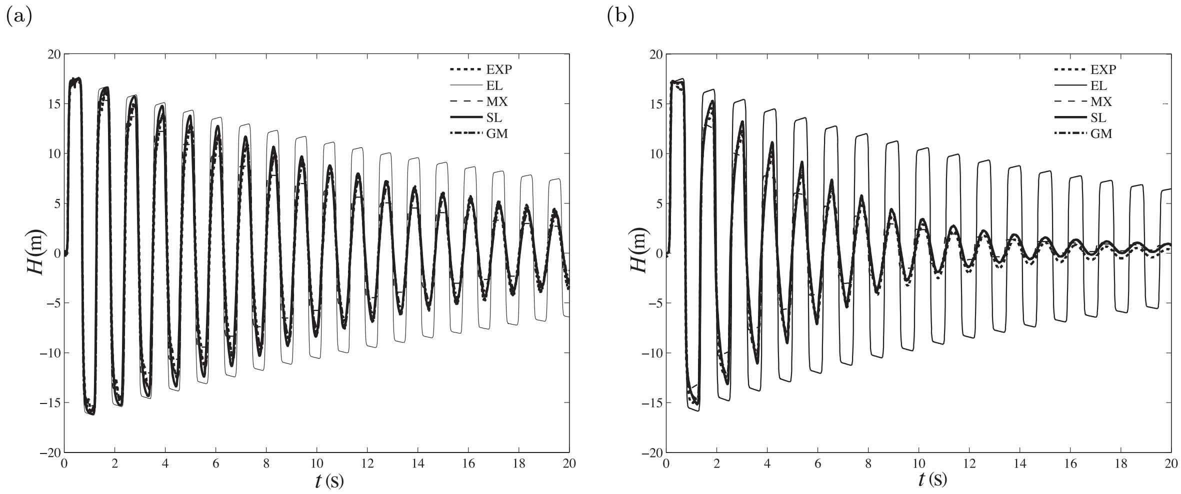

Figure 9: Comparison of the measured and simulated values of H at $\mathrm{PT_D}$ for (a) PVC-O and (b) HDPE.

periodicity is captured by the estimated wave speed, the peaks shape and the signal damping cannot be modeled using only one parameter. The comparison of Figs 5a and 5b and the obtained values of σ^2 confirm that PVC-O behaves more as an elastic material than HDPE, at least in the considered test conditions.

Figures 9 and 10 show that MX reproduces the periods and the squared shape of the oscillations of EL, but the added parameter allows to explain the damping of the peaks due to the viscoelasticity for both PVC-O and HDPE. The limits in the use of this model were expected, since it is well known that the MX model cannot properly reproduce the creep of the material. Nevertheless it is worth of noting how the introduction of one parameter significantly improves the numerical modeling.

The use of three parameters for SL and GM increases the performance of the numerical simulations. These models capture the damping better than EL and MX and the simulated signals resemble the experimental ones also in the rounded shape of the peaks over the long duration, typical of transients in viscoelastic pipes. The fractional derivatives implemented in GM work better than the integer order derivatives of SL, both for PVC-O and HDPE, although the differences in terms of σ^2 are small. The shown dependence of σ^2 on the parameters and the limited range of variation of θ suggest possible advantages in the calibration of GM with respect to SL.

Assuming that θ gives a measure of the viscous behavior of a material, the calibrated values confirm the "weak" viscoelastic behavior of the PVC-O.

To assess the reliability of the optimal set of the estimated parameters, the same numerical

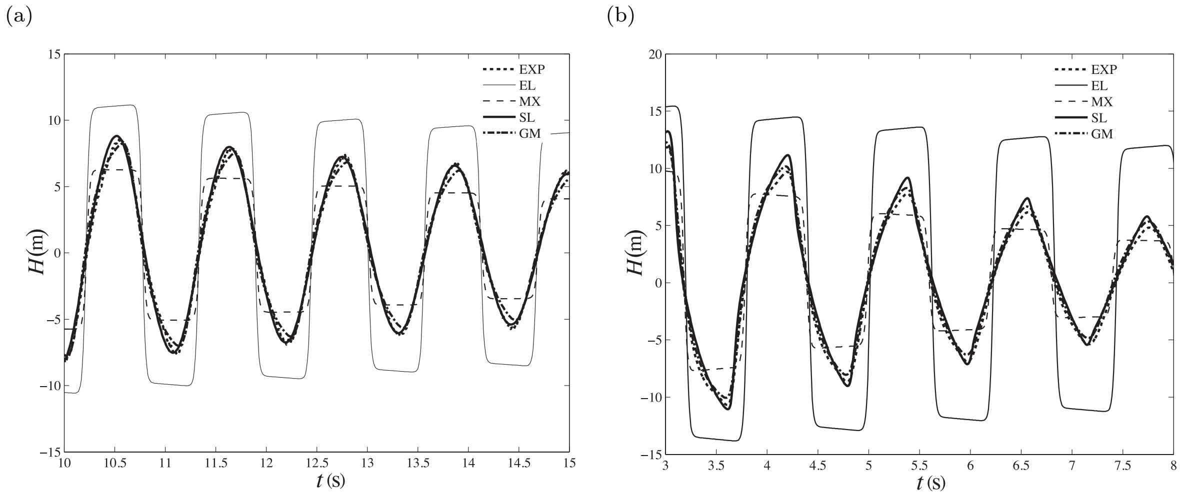

Figure 10: Comparison of the measured and simulated values of H at PT_D for (a) PVC-O and (b) HDPE. The same signals of Fig. 9 are plotted in a narrower time interval to enhance the comparison of the models over the long durations.

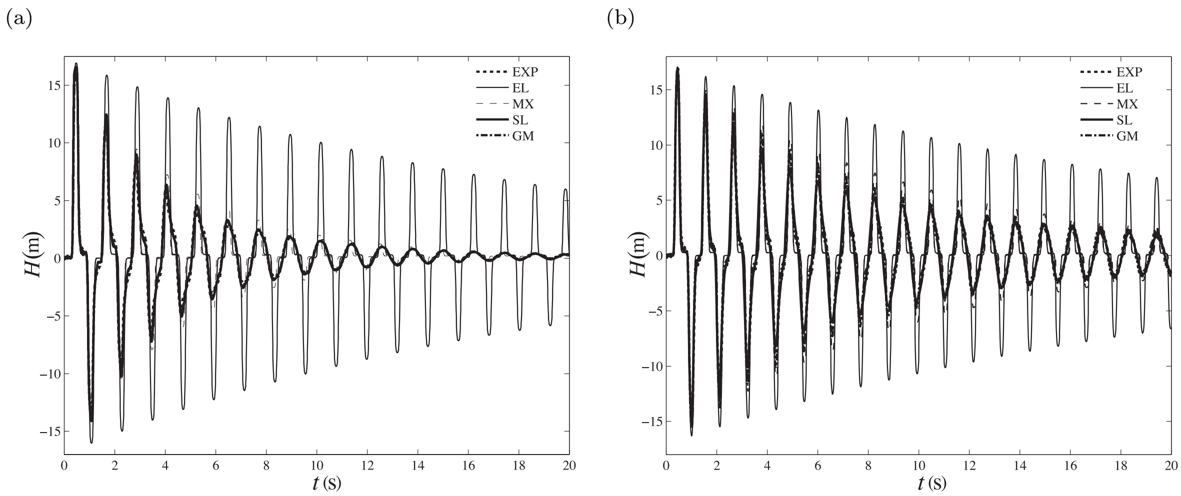

Figure 11: Comparison of the measured and simulated values of H at PT_{IU} for (a) PVC-O and (b) HDPE.

models reproducing the experimental data at PT_D with the minimum of σ^2 are used in Figs 11 and 12 and compared to the experimental signals at PT_{IU}. Although the optimization of the parameters is obtained on the experimental data at PT_D, the obtained sets of parameters are adequate to reproduce the data also at this other section, with a comparable accuracy. All the comments regarding the comparison of simulated and experimental data at PT_D apply also at PT_{IU}, validating the optimization procedure and the results.

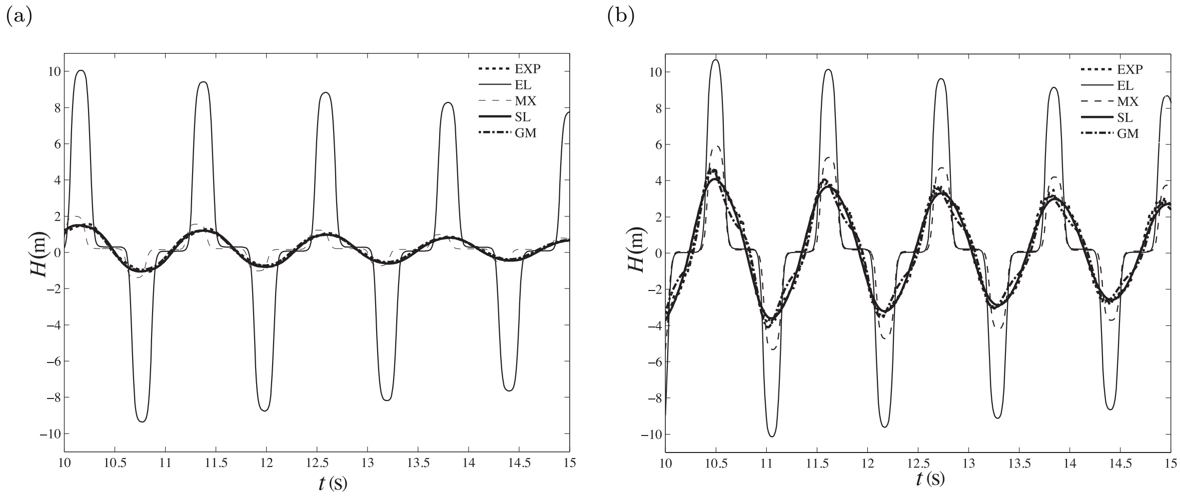

Figure 12: Comparison of the measured and simulated values of H at $\mathrm{PT_{IU}}$ for (a) PVC-O and (b) HDPE. The same signals of Fig. 11 are plotted in a narrower time interval to enhance the comparison of the models over the long duration.

7 Conclusions

In this paper, the reliability of different viscoelastic models in reproducing experimental data acquired during transient tests is analyzed for two polymeric pipe materials with a different rheological behavior, that are PVC-O and HDPE. The parameters of the viscoelastic models are calibrated and the results are compared. The calibration procedure is performed by means of a frequency domain model, which allows a fast and reliable simulation of transients. Furthermore, the implementation of the viscoelastic models is easier with respect to the time domain models and does not require any linearization.

The sum of the squared residuals between experimental data and numerical results, expressed by σ^2, is used as the optimization function and it is analyzed in the space of the parameters. This choice is suggested by the large use of this function in statistics and information theory. With reference specifically to transient tests, it is directly or indirectly used by almost all of the authors in the calibration procedures and can be considered as a standard practice. The shape of the optimization function is shown for the models to give an insight into the sensitivity of the calibration to the parameters.

The results of the calibrations point out the limits of σ^2 as optimization function and the need of defining other optimization functions that take into account some peculiar aspects of the transient pressure signals, such as the number of periods and the damping of the maxima. As an example, if only the maxima and minima of the pressure signals are considered, the MX model can be considered reliable as the others, with a reduced number of parameters. Furthermore, based on σ^2, a numerical model reproducing with a completely wrong period the experimental data could be considered more reliable than one reproducing the correct period.

The introduced viscoelastic model GM, based on fractional derivatives, performs slightly better than the well known SL, for both HDPE and PVC-O, although the differences in terms of σ^2 are small. Nevertheless, the calibration reliability and speed can take advantage from the shape of the optimization function of the GM, thus encouraging its use. It is worth of noticing that the parameter θ represents also a simple measure of the degree of viscosity (or elasticity) of the pipe material.

Several issues raised by the present investigation need to be further addressed. As an example, attention should be paid to the use of an optimization function suited for transient tests, which penalizes the calibrated models out of phase and helps in the comparison of the main transient characteristics, such as peak values or damping. Further work is also needed to compare models with a different number of parameters and to assess if the increase in the number of the parameters can be justified by the improvement in the description of the experimental data or it represents just an overfitting. Additional efforts are needed to confirm that the advantages in using the fractional derivatives are meaningful as put forward by the presented results.

Acknowledgements

This research has been supported by the University of Perugia and by the Italian Ministry of Education, University and Research (MIUR) — under the Project of Relevant National Interest "Tools and procedures for an advanced and sustainable management of water distribution systems".

References

Bagley, R. L. (1986). On the fractional calculus model of viscoelastic behavior. *Journal of Rheology*, *30*(1), 133–24.

Bagley, R. L., & Torvik, P. J. (1983). A theoretical basis for the application of fractional calculus to viscoelasticity. *Journal of Rheology*, *27*(3), 201–11.

Bergant, A., Simpson, A. R., & Vítkovský, J. P. (2001). Developments in unsteady pipe flow friction modelling. *Journal of Hydraulic Research, IAHR*, *39*(3), 249–257.

Brunone, B., Golia, U. M., & Greco, M. (1995). Effects of two-dimensionality on pipe transients modeling. *Journal of Hydraulic Engineering, ASCE*, *121*(12), 906–912.

Brunone, B., & Morelli, L. (1999). Automatic control valve induced transients in an operative pipe system. *Journal of Hydraulic Engineering, ASCE*, *125*(5), 534–542.

Capponi, C., Zecchin, A. C., Ferrante, M., & Gong, J. (sub). Numerical study on accuracy improvement of linearized impulse-response modeling of transients in smooth pipes. *Journal of Hydraulic Research, IAHR.*

Caputo, M., & Mainardi, F. (1971). A new dissipation model based on memory mechanism. *Pure and Applied Geophysics*, *91*(1), 134–147.

Cassa, A. M., van Zyl, J. E., & Laubscher, R. (2010). A numerical investigation into the effect of pressure on holes and cracks in water supply pipes. *Urban Water Journal*, *7*(2), 109–120.

Chaudhry, M. H. (2014). *Applied Hydraulic Transients* (Third ed.). New York, NY: Springer New York.

Covas, D. I. C., Stoianov, I., Mano, J., Ramos, H., Graham, N., & Maksimovic, C. (2005). The dynamic effect of pipe-wall viscoelasticity in hydraulic transients. Part II - model development, calibration and verification. *Journal of Hydraulic Research, IAHR*, *43*(1), 56–70.

Covas, D. I. C., Stoianov, I., Ramos, H., Graham, N., Maksimovic, C., & Butler, D. (2004). Water hammer in pressurized polyethylene pipes: conceptual model and experimental analysis. *Urban Water Journal*, *1*(2), 177–197.

Di Paola, M., Pirrotta, A., & Valenza, A. (2011). Visco-elastic behavior through fractional calculus: An easier method for best fitting experimental results. *Mechanics of Materials*, *43*(12), 799–806.

Duan, H.-F., Ghidaoui, M., & Lee, P. J. (2010). Unsteady friction and visco-elasticity in pipe fluid transients. *Journal of Hydraulic Research, IAHR*, *48*(3), 354–362.

Duan, H.-F., Lee, P. J., Ghidaoui, M. S., & Tung, Y.-K. (2012). System Response Function–Based Leak Detection in Viscoelastic Pipelines. *Journal of Hydraulic Engineering, ASCE*, *138*(2), 143–153.

Evangelista, S., Leopardi, A., Pignatelli, R., & de Marinis, G. (2015). Hydraulic Transients in Viscoelastic Branched Pipelines. *Journal of Hydraulic Engineering, ASCE*, *141*(8), 04015016–9.

Ferrante, M. (2012). Experimental investigation of the effects of pipe material on the leak head-discharge relationship. *Journal of Hydraulic Engineering, ASCE*, *138*(8), 736–743.

Ferrante, M., & Brunone, B. (2003). Pipe system diagnosis and leak detection by unsteady-state tests. 1. Harmonic analysis. *Advances in Water Resources*, *26*(1), 95–105.

Ferrante, M., Capponi, C., Brunone, B., & Meniconi, S. (2015). Hydraulic characterization of PVC-O pipes by means of transient tests. *Procedia Engineering*, *119*, 263–269.

Ferrante, M., Massari, C., Brunone, B., & Meniconi, S. (2011). Experimental evidence of hysteresis in the head-discharge relationship for a leak in a polyethylene pipe. *Journal of Hydraulic Engineering, ASCE*, *137*, 775–780.

Fox, S. (2016). *Understanding the dynamic leakage behaviour of longitudinal slits in viscoelastic pipes* (Unpublished doctoral dissertation). The University of Sheffield.

Ghilardi, P., & Paoletti, A. (1987). Viscoelastic parameters for the simulation of hydraulic transients in polymeric pipes. *Excerpta*, *2*, 51-62.

Gong, J., Zecchin, A. C., Lambert, M. F., & Simpson, A. R. (2016). Determination of the creep function of viscoelastic pipelines using system resonant frequencies with hydraulic transient analysis. *Journal of Hydraulic Engineering, ASCE*, 04016023.

Gorenflo, R., & Mainardi, F. (2007). Time-fractional derivatives in relaxation processes: A tutorial survey. *Fractional Calculus and Applied Analysis*, *10*(3), 269–308.

Kim, S. H. (2005). Extensive development of leak detection algorithm by impulse response method. *Journal of Hydraulic Engineering, ASCE*, *131*, 201.

Kim, S. H. (2007). Impedance matrix method for transient analysis of complicated pipe networks. *Journal of Hydraulic Research, IAHR*, *45*(6), 818–828.

Kim, S. H. (2016). Impedance method for abnormality detection of a branched pipeline system. *Water Resources Management*, *30*(3), 1101–1115.

Kim, S. H., Zecchin, A. C., & Choi, L. (2014). Diagnosis of a pipeline system for transient flow in low reynolds number with impedance method. *Journal of Hydraulic Engineering, ASCE*, *140*(12), 04014063–10.

Lee, P. J. (2013). Energy analysis for the illustration of inaccuracies in the linear modelling of pipe fluid transients. *Journal of Hydraulic Research, IAHR*, *51*(2), 133–144.

Lee, P. J., Duan, H.-F., Ghidaoui, M., & Karney, B. (2013). Frequency domain analysis of pipe fluid transient behaviour. *Journal of Hydraulic Research, IAHR*, *51*(6), 609–622.

Lee, P. J., Duan, H.-F., Tuck, J., & Ghidaoui, M. (2015). Numerical and experimental study on the effect of signal bandwidth on pipe assessment using fluid transients. *Journal of Hydraulic*

Engineering, ASCE, *141*(2), 04014074 1–04014074 7.

Lee, P. J., & Vítkovský, J. P. (2010). Quantifying linearization error when modeling fluid pipeline transients using the frequency response method. *Journal of Hydraulic Engineering, ASCE*, *136*(10), 831–836.

Mainardi, F. (2010). *Fractional calculus and waves in linear viscoelasticity.* Imperial College Press.

Massari, C., Ferrante, M., Brunone, B., & Meniconi, S. (2012). Is the leak head–discharge relationship in polyethylene pipes a bijective function? *Journal of Hydraulic Research, IAHR*, *50*(4), 409–417.

Pezzinga, G. (2000). Evaluation of unsteady flow resistances by quasi-2D or 1D models. *Journal of Hydraulic Engineering, ASCE*, *126*(10), 778–785.

Pezzinga, G., Brunone, B., Cannizzaro, D., Ferrante, M., Meniconi, S., & Berni, A. (2014). Two-dimensional features of viscoelastic models of pipe transients. *Journal of Hydraulic Engineering, ASCE*, 04014036–1–04014036–9.

Pezzinga, G., & Scandura, P. (1995). Unsteady flow in installations with polymeric additional pipe. *Journal of Hydraulic Engineering, ASCE*, *121*(11), 802–811.

Schiessel, H., & Blumen, A. (1993). Hierarchical analogues to fractional relaxation equations. *Journal of Physics A: Mathematical and General*, *26*(19), 50-57.

Schiessel, H., & Blumen, A. (1995). Mesoscopic pictures of the sol-gel transition: Ladder models and fractal networks. *Macromolecules*, *28*(11), 4013–4019.

Shimizu, N., & Zhang, W. (1999). Fractional calculus approach to dynamic problems of viscoelastic materials. *JSME International Journal, Series C: Mechanical Systems, Machine Elements and Manufacturing*, *42*(4), 825–837.

Soares, A. K., Covas, D. I., & Reis, L. F. (2008). Analysis of PVC pipe-wall viscoelasticity during water hammer. *Journal of Hydraulic Engineering, ASCE*, *134*(9), 1389-1394.

Soares, A. K., Covas, D. I. C., & Reis, L. F. (2011). Leak detection by inverse transient analysis in an experimental PVC pipe system. *Journal of Hydroinformatics*, *13*(2), 153-166.

Ssozi, E. N., Reddy, B. D., & van Zyl, J. E. (2016). Numerical investigation of the influence of viscoelastic deformation on the pressure-leakage behavior of plastic pipes. *Journal of Hydraulic Engineering, ASCE*, *142*(3), 04015057–1 – 04015057–9.

Suo, L., & Wylie, E. B. (1989). Impulse response method for frequency-dependent pipeline transients. *Journal of Fluids Engineering*, *111*(4), 478–483.

Tijsseling, A. S. (1996). Fluid-structure interaction in liquid-filled pipe systems: a review. *Journal of Fluids and Structures*, *10*(2), 109–146.

Tijsseling, A. S., & Vardy, A. (2015). What is wave speed? In A. S. Tijsseling (Ed.), *12 th international conference pressure surges* (pp. 343–360).

van Zyl, J. E., & Cassa, A. M. (2013). Modeling elastically deforming leaks in water distribution pipes. *Journal of Hydraulic Engineering, ASCE*, *140*(2), 182–189.

Vítkovský, J. P., Lee, P., Zecchin, A. C., Simpson, A. R., & Lambert, M. F. (2011). Head- and flow-based formulations for frequency domain analysis of fluid transients in arbitrary pipe networks. *Journal of Hydraulic Engineering, ASCE*, *137*(5), 556–568.

Weinerowska-Bords, K. (2006). Viscoelastic model of waterhammer in single pipeline-problems and questions. *Archives of Hydro-Engineering and Environmental Mechanics*, *53*(4), 331–351.

Weinerowska-Bords, K. (2015). Alternative approach to convolution term of viscoelasticity in equations of unsteady pipe flow. *Journal of Fluids Engineering*, *137*(5), 054501–1 – 054501–9.

Wylie, E. B., & Streeter, V. (1993). *Fluid transients in systems.* Eaglewood Cliffs, New Jersey, USA: Prentice-Hall, Inc.

Zecchin, A. C., Lambert, M. F., & Simpson, A. R. (2010). Frequency-domain modeling of transients in pipe networks with compound nodes using a Laplace-domain admittance matrix. *Journal of Hydraulic Engineering, ASCE*, *136*(10), 739–755.

Zecchin, A. C., Simpson, A. R., & Lambert, M. F. (2009). Transient modeling of arbitrary pipe networks by a Laplace-domain admittance matrix. *Journal of Engineering Mechanics, ASCE*, *135*(6), 538-547.